ISOPYCNIC PHASES AND STRUCTURES IN H_2O/CO_2/ETHOXYLATED ALCOHOL SURFACTANT MIXTURES

Michael E. Paulaitis
Department of Chemical Engineering
Johns Hopkins University
Baltimore, MD 21218

Richard G. Zielinski and Eric W. Kaler
Center for Molecular and Engineering Thermodynamics
Department of Chemical Engineering
University of Delaware
Newark, Delaware 19716

54-25
S-167

ABSTRACT

Ternary mixtures of H_2O and CO_2 with ethoxylated alcohol (C_iE_j) surfactants can form three coexisting liquid phases at conditions where two of the phases have the same density (isopycnic phases). Isopycnic phase behavior has been observed for mixtures containing the surfactants C_8E_5, $C_{10}E_6$, and $C_{12}E_6$, but not for those mixtures containing either C_4E_1 or C_8E_3. Pressure-temperature (PT) projections for this isopycnic three-phase equilibrium were determined for $H_2O/CO_2/C_8E_5$ and $H_2O/CO_2/C_{10}E_6$ mixtures at temperatures from approximately 25 to 33°C and pressures between 90 and 350 bar. As a preliminary to measuring the microstructure in isopycnic three component mixtures, phase behavior and small angle neutron scattering (SANS) experiments were performed on mixtures of $D_2O/CO_2/$ n-hexaethyleneglycol monododecyl ether ($C_{12}E_6$) as a function of temperature (25-31°C), pressure (63.1-90.7 bar), and CO_2 composition (0-3.9 wt%). Parameters extracted from model fits of the SANS spectra indicate that, while micellar structure remains essentially unchanged, critical concentration fluctuations increase as the phase boundary and plait point are approached.

INTRODUCTION

Surfactant solutions containing near-critical or supercritical fluids that form equilibrium phases of equal density (isopycnic phases) are uniquely suited for simulating phase separation in microgravity environments where density differences between the separating phases are irrelevant. For compressible supercritical-fluid mixtures, pressure becomes an additional field variable with which to adjust and control phase boundaries.[1-3] As a consequence, rapid pressure quenches can be made to access metastable or unstable regions of the phase diagram, thereby permitting the convenient study of phase separation dynamics and mechanisms. In addition, low interfacial tensions and the presence of colloidal microstructure in surfactant-containing mixtures[1, 3-5] retard phase separation. In this work, isopycnic phase behavior for three-phase, liquid-liquid-liquid (L1-L2-L3) equilibrium was investigated for ternary mixtures of H_2O and CO_2 with the ethoxylated alcohol (C_iE_j) surfactants: C_4E_1, C_8E_3, C_8E_5, $C_{10}E_6$, and $C_{12}E_6$. CO_2 was chosen for study because it has a readily accessible critical point (31.06°C and 73.825 bar) and a reasonably high critical density (0.4660 g/cm^3).[6]

Surfactant self-assembly in near-critical or supercritical fluids opens the possibility that pressure or fluid density could also be used to alter surfactant microstructure.[7, 8] Most prior studies of surfactant microstructure in solutions containing supercritical or near-critical fluids have focused on the supercritical fluid-rich corner of the phase diagram, where the effects of pressure on microstructure and phase behavior are expected to be large. Here we use small angle neutron scattering experiments to examine the effect of carbon dioxide on the interactions, critical fluctuations, and structure of $C_{12}E_6/D_2O$ micellar mixtures in the water-rich corner of the phase diagram. The scattering spectra are successfully modeled using a polydisperse hard sphere form factor to determine particle shape and size, together with an Ornstein-Zernike structure factor to quantify the critical phenomena. Using the model parameters, the micellar composition was calculated to determine the

partitioning of carbon dioxide between the water and the micelles.[9]

EXPERIMENTAL SECTION

Observations of isopycnic phase behavior were made using a variable-volume view cell. The cell design and experimental technique are described in detail elsewhere.[1] The view cell is a sapphire tube (Insaco) 17.78 cm long with an inner diameter of 1.113 ± 0.001 cm and an outer diameter of 1.67 cm. It is sealed internally on each end with Viton O-rings and Polymite backing rings mounted on stainless steel endcaps. The endcaps are held in place against the internal cell pressure by a C-bracket that also provides support for the sapphire tube. The cell in this configuration was hydrostatically tested to 551 bar. The view cell is also equipped with a movable piston to allow pressure to be varied independently of sample composition and temperature. Pressure in the cell is generated using a water-filled syringe pump (High Pressure Equipment) to move the piston and compress the sample. Two spring-loaded seals (Bal-Seal Engineering) near each end of the piston insure proper alignment of the piston in the sapphire tube and separate the pressurizing fluid from the surfactant solution. Sample pressure is determined indirectly by measuring the pressure of the pressurizing fluid to within ± 0.5 bar with a Bourdon tube gauge (Heise). The pressure drop across the piston was determined to be less than 1-2 bar at 300 bar. The entire assembly is immersed in a high precision water bath (Hart Scientific), which controlled temperature to ± 0.001°C. The temperature of the bath is measured with an NBS mercury thermometer (± 0.005 °C). The custom-designed temperature bath has a window for phase behavior observations.

The L1 and L2 phase densities were measured to a maximum accuracy of ± 10^{-5} g/cm^3 using a vibrating tube densimeter and the method of Kratky *et al.*[10] The densimeter (Anton-Paar DMA-512 rated to 400 bar) was calibrated at each temperature and pressure with nitrogen and water. Sample was transferred from the view cell to the densimeter using the movable piston as a syringe to displace the fluid. Sampling of a particular phase was facilitated by loading the view cell such that this phase was present in excess. Constant pressure (± 3 bar) was maintained during sampling by filling the densimeter and all transfer lines with nitrogen to the pressure of the view cell. The densimeter temperature was controlled to ± 0.05°C by recirculating water from the temperature bath for the view cell. The pressure in the densimeter was measured directly to within ± 0.3 bar with a Bourdon tube gauge (Heise).

Densities of the surfactant/water solutions at ambient pressure were measured using a second vibrating tube densimeter (Anton-Paar DMA 602) with a maximum accuracy of ± 10^{-6} g/cm^3. The densimeter temperature in these experiments was controlled to ± 0.1°C by an external temperature bath (Neslab RTE 111) and was measured to ± 0.02 °C using a quartz thermometer (Hereaus Sensor) immersed in the bath. Solutions were injected manually into the densimeter.

The non-ionic surfactants C_8E_3, C_8E_5 (Bachem and Biosciences, >98% pure C_8E_5), $C_{12}E_6$, $C_{10}E_6$ (Nikko, >99% pure), and C_4E_1 (Aldrich, >99% pure) were used as received. Water was distilled, deionized, and degassed of oxygen to minimize surfactant degradation over the course of the experiment. Carbon dioxide (Matheson, Coleman Grade, >99.99% pure) and nitrogen (Airco, high pressure, 99.998% pure) were used as received.

Small-angle neutron scattering was performed using the 30 meter spectrometer at the National Institute of Standards and Technology (NIST), in Gaithersburg, MD. Neutrons with a 5 Å wavelength ($\Delta\lambda/\lambda = 0.15$) gave q-values from 0.007 to 0.22 Å^{-1} where q, the magnitude of the scattering vector, is defined as $q = (4\pi/\lambda)\sin(\theta/2)$ and θ is the scattering angle. Data were put on absolute scale using a silica standard and data handling software supplied by NIST, and corrected for scattering from the empty cell and the D_2O solvent. The high pressure SANS cell is made entirely of machined sapphire (Insaco Inc.) to facilitate measuring at large (30 degree) scattering angles. The scattering cell has a path length of 2mm and a total volume of 1.6 ml, and is thermostated by an aluminum heat transfer jacket. Temperature was measured with a platinum RTD (Newport Electronics, ± 0.1 C) placed inside the scattering cell. Liquid-tight sealing at the ends of the SANS cell was accomplished with viton O-Rings (Parker size 2-013) and backing rings (Parker size 8-013) mounted on stainless steel endcaps.

RESULTS

Three equilibrium phases were observed for mixtures of H_2O, CO_2, and C_8E_5 at 25.5 to 30.0°C and 91 to 360 bar. The water-rich L1 phase and the surfactant-rich L2 phase were identified from the known overall composition of the mixture and the observed relative volumes of the two phases. The CO_2-rich L3 phase was found to have the lowest density at all conditions studied. The measured L1 and L2 phase densities at 30.0°C are shown in Figure 1 as a function of pressure. At low pressures, the L1 phase has a higher density than the L2 phase, and at higher pressures, the L2 phase density is higher. The pressure at which the two densities are equal (the isopycnic pressure) is 308 ± 3 bar, which is given by the intersection of the two linear fits to the densities near the isopycnic pressure. An experimental uncertainty of ± 3 bar is estimated from uncertainties in the pressure (± 2 bar) and the density (± 10^{-4} g/cm^3) measurements. The observed inversion of the L1 and L2 phases at this temperature was found to be within ± 7 bar of this value.

Isopycnic pressures at other temperatures and for ternary mixtures of H_2O, CO_2, and $C_{10}E_6$ were determined only from observations of the L1-L2 phase inversion. The pressure-temperature (PT) projections for this isopycnic three-phase, L1-L2-L3 equilibrium are shown in Figure 2. These two projections are similar with the one for $C_{10}E_6$-containing mixtures shifted to higher temperatures by approximately 2°C. In both cases, the isopycnic pressure increases dramatically with increasing temperature. The L1-L2 phase inversion was also observed for $H_2O/CO_2/C_{12}E_6$ mixtures in L1-L2-L3 equilibrium at 18.6°C and approximately 394 bar. However, the ternary mixtures containing either C_4E_1 or C_8E_3 did not exhibit an inversion at a temperature of 26.9°C and pressures between 90 to 310 bar.

Phase boundaries between one- and two-phase regions for mixtures of D_2O/ CO_2/ $C_{12}E_6$ were determined at constant pressure and composition by measuring the temperature where the mixture became turbid.[9] Figure 3 shows the temperature-CO_2 concentration phase diagrams at 63.1 and 90.7 bar for a constant D_2O to $C_{12}E_6$ weight ratio of 12.8 to 1. Carbon dioxide at small concentrations depresses the coexistence curve in $C_{12}E_6/D_2O$ mixtures by more than 20 °C at 4.3 wt% CO_2. The phase boundary changes little from 63.1 to 90.7 bar, increasing a maximum of 0.52°C at 4.3 wt% CO_2.

SANS measurements were made on mixtures of $C_{12}E_6$, CO_2, and D_2O in the one- phase region in the water-rich corner of the phase diagram (7.5 wt% $C_{12}E_6$ on a CO_2-free basis) containing varying amounts of carbon dioxide. The compositions of the samples examined by SANS are represented by the crosses in Figure 3. SANS experiments are reported in detail elsewhere[9] were performed at 63.1, 76.9, and 90.7 bar and temperatures of 25, 28, and 31°C in order to span the carbon dioxide critical pressure near its critical temperature. As an example of the results, scattering spectra and model descriptions (solid lines) for the samples at 31°C and 63.1 bar are shown on log-log scales in Figure 4 as plots of neutron scattered intensity on an absolute scale as a function of the magnitude of the scattering vector, q. For clarity of presentation, some of the spectra are multiplied by 2 or 4 (shown as (x2) or (x4) in the figure caption) to be offset from the other spectra. These spectra are distinguished by different degrees of upturn at low q. This feature usually arises from the presence of either attractive interactions between micelles or critical scattering. The high q portions of the spectra change little in shape with changes in temperature, pressure, or CO_2 composition. This indicates that the micelle structure does not change under these conditions.

DISCUSSION

Mixtures of H_2O and CO_2 with either C_8E_5 or $C_{10}E_6$ form isopycnic L1 and L2 phases in three-phase, liquid-liquid-liquid equilibrium at elevated pressures and temperatures in the range of 25 - 35°C (Figure 2). The effect of pressure is to increase the density of the L2 phase to a greater extent than that of the L1 phase (Figure 1), which leads to the observed isopycnic phase behavior. The higher compressibility of the L2 phase can be attributed at least in part to the higher pure-component compressibilities of both the surfactant and CO_2. However, the L1 phase densities are always greater

than the densities of each of the three pure components for the temperatures and pressures studied. Thus, the L2 phase density will always be less than that for the water-rich L1 phase if these components formed ideal mixtures at the conditions studied. It follows, therefore, that non-ideal mixing must account for the existence of isopycnic phases.

Non-ideal mixing in the form of negative excess molar volumes has been determined experimentally for binary mixtures of C_8E_5 with CO_2 and with H_2O. Excess molar volumes for binary mixtures of CO_2 and H_2O, calculated from measured liquid densities at 26°C, are likewise negative.[11, 12] For example, Francis[11] reports a partial molar volume of 32.4 cc/mole for CO_2 in water at 26°C and 66.0 bar, which is much less than the liquid molar volume of pure CO_2 at these conditions (65.8 cm^3/mol). The measured pressure dependence of CO_2 solubilities in water[13] gives similar values for the partial molar volume of CO_2 in water, indicating negative excess molar volumes for this binary mixture.

Liquid densities for ternary H_2O/ CO_2/ C_8E_5 mixtures can be predicted from measured densities for the binary mixtures using a recent modification of the Peng-Robinson equation of state (PR EOS).[14] In this modification, the original form of the equation for mixtures and the conventional quadratic mixing rules have been retained, but the combining rule for the a_{ij} parameters when $i \neq j$ is modified to incorporate an additional adjustable parameter for each pair of constituents. This PR EOS provides an accurate description of highly non-ideal thermodynamic behavior over the entire range of mixture compositions.

Turning now to microstructure studies, the scattering spectra of D_2O/ $C_{12}E_6$ mixtures show an upturn at low q as a function of CO_2 concentration (Figure 4). To model the spectra, we assume there is no correlation between particle size and interactions. For this case, the effects of particle shape (form factor) and interactions (structure factor) on the measured intensity can be determined independently. The model intensity as a function of q can be written as:

$$\frac{d\Sigma}{d\Omega} = (\Delta\rho)^2 \phi V \langle P(q) \rangle S(q) + B \qquad (1)$$

where $(\Delta\rho)^2\phi$ is the product of contrast and volume fraction of particles, V is the volume of a micelle, $\langle P(q) \rangle$ is the form factor normalized by $1/V^2$, S(q) is the structure factor, which depends on the correlation length ξ, and B represents the incoherent scattering background.

Because of the shape of the scattering curves and the proximity of the sample composition, pressure, and temperature to the phase boundary, a modified Ornstein-Zernike structure factor together with a form factor for polydisperse spheres were chosen to model the data. The form factor assumes a Schultz distribution for the particle radii and includes particle radius and the Schultz width parameter (a measure of the degree of polydispersity) as parameters.[15] The use of a form factor that accounts for polydispersity together with a structure factor that assumes a monodisperse population of aggregates is a good approximation for polydisperse hard spheres when the ratio of polydispersity to radius is less than 0.3.[16] The modified Ornstein-Zernike structure factor is $S(q) = 1 + S(0) / [1 + (q\xi)^2]$.

The values for the five fitted parameters: radius (r), polydispersity, correlation length (ξ), S(0), and $(\Delta\rho)^2\phi$ were determined by minimizing the χ^2 value between the model fit and the experimental data. The fits of the five parameter model to the data are excellent except at the highest values of q, which reflects the assumption that the incoherent background remains constant through all of the fitting. The fitting shows that the micelle size remains constant at about 50 Å diameter, while the correlation length increases from 70 to 110 Å as CO_2 concentration increases from 0 to 3.9 wt% (Figure 4). Analysis of $(\Delta\rho)^2\phi$ shows that, for the 3.9 wt% CO_2 samples no more than 7% of the added carbon dioxide enters the micelles.

CONCLUSIONS

Phase behavior observations show that isopycnic liquid phases form in ternary mixtures of $H_2O/CO_2/C_8E_5$, $C_{10}E_6$, or $C_{12}E_6$, but not in mixtures of $H_2O/CO_2/C_4E_1$ or C_8E_3. Isopycnic phase formation is favored by raising the pressure or decreasing the temperature. At elevated pressures, this phase behavior is due in large part to favorable changes in the L2 phase composition for three-phase, liquid-liquid-liquid equilibrium. Non-ideal mixing effects that lead to a density maximum for the H_2O/CO_2 binary mixture are necessary for the formation of isopycnic phases in these ternary mixtures.

SANS measurements on the system $D_2O/CO_2/C_{12}E_6$ in the water-rich corner of the phase diagram indicate the presence of spherical micelles ca. 50 Å in diameter. This dimension is similar to that of micelles formed in mixtures of D_2O and $C_{12}E_6$ alone. Micelle structure does not change over the range of pressures, temperatures, and compositions studied. The increase in S(0) and ξ are consistent with increasing critical concentration fluctuations caused by the approach of a plait point and the phase boundary. Analysis of the product $(\Delta\rho)^2\phi$ as a function of carbon dioxide density and concentration indicates that little or no carbon dioxide added to the solution partitions into the micelles.

ACKNOWLEDGMENTS

This work was supported by the National Aeronautics and Space Administration (NAG3-1424) and a NASA graduate student researcher program fellowship for R. G. Z. We acknowledge the support of the National Institute of Standards and Technology, U.S. Department of Commerce, in providing the facilities used in this experiment. The assistance of John Barker and Charlie Glinka during the SANS experiments is gratefully acknowledged, as are helpful discussions with Steve Kline, Y. Jayalakshmi, K.-V. Schubert, and C.-P. Chai Kao.

REFERENCES

1. J. M. Ritter and M. E. Paulaitis, Langmuir *6*, 934-941 (1990).
2. G. J. McFann and K. P. Johnston, Langmuir *9*, 2942-2948 (1993).
3. G. J. McFann, K. P. Johnston and S. M. Howdle, AIChE J. *40*, 543-555 (1994).
4. E. W. Kaler, J. F. Billman, J. L. Fulton and R. D. Smith, Journal of Physical Chemistry *95*, 458-462 (1991).
5. J. M. Tingey, J. L. Fulton, D. W. Matson and R. D. Smith, Journal of Physical Chemistry *95*, 1443-1448 (1991).
6. "*Carbon Dioxide International Thermodynamic Properties of the Fluid State -3*"; S. Angus, B. Armstrong and K. M. d. Reuk, Eds.; Pergamon Press: Oxford, 1976.
7. J. L. Fulton and R. D. Smith, Journal of Physical Chemistry *92*, 2903-2907 (1988).
8. R. W. Gale, J. L. Fulton and R. D. Smith, Journal of the American Chemical Society *109*, 920-921 (1987).
9. R. G. Zielinski, E. W. Kaler and M. E. Paulaitis, Journal of Physical Chemistry *99*, 10354-10358 (1995).
10. O. Kratky, H. Leopold and H. Stabinger, Z. Angew. Phys. *27*, 273 (1969).
11. A. W. Francis, Journal of Physical Chemistry *58*, 1099-1114 (1954).
12. T. Ohsumi, N. Nakashiki, K. Shitashima and K. Hirama, Energy Conserv. Mgmt. *33*, 685-690 (1992).
13. W. J. Parkinson and N. DeNevers, I&EC Fundamentals*8*, 709-713 (1969).
14. C.-P. C. Kao, M. E. Paulaitis, G. A. Sweany and M. Yokozeki, Fluid Phase Equilibria *108*, 27-46 (1995).
15. M. Kotlarchyck and S. H. Chen, Journal of Chemical Physics *79*, 2461-2469 (1983).
16. W. L. Griffith, R. Triolo and A. L. Compere, Physical Review A *35*, 2200-2206 (1987).

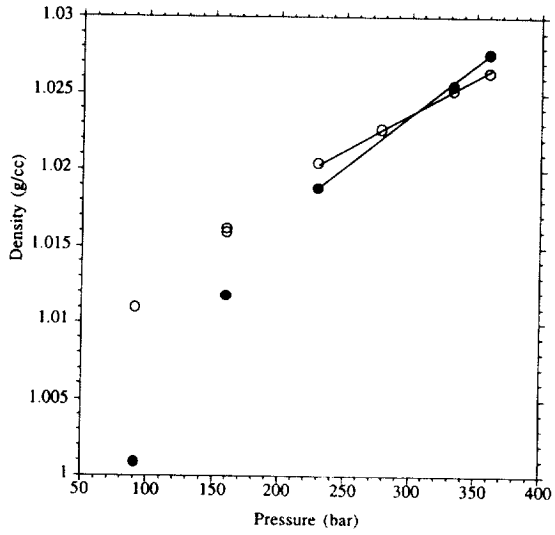

Figure 1. Measured densities of the L1 phase (open circles) and the L2 phase (closed circles) in three-phase, liquid-liquid-liquid equilibrium as a function of pressure at 30.0°C for $H_2O/CO_2/C_8E_5$ ternary mixtures. The linear interpolations of the data define the isopycnic pressure at 308 bar.

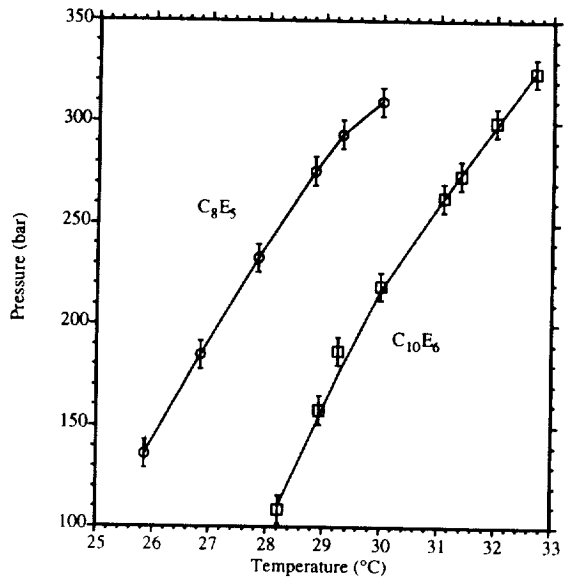

Figure 2. Measured pressure-temperature projections for isopycnic L1 and L2 phases in three-phase equilibrium for $H_2O/CO_2/C_8E_5$ (circles) and $H_2O/CO_2/C_{10}E_6$ (squares) ternary mixtures.

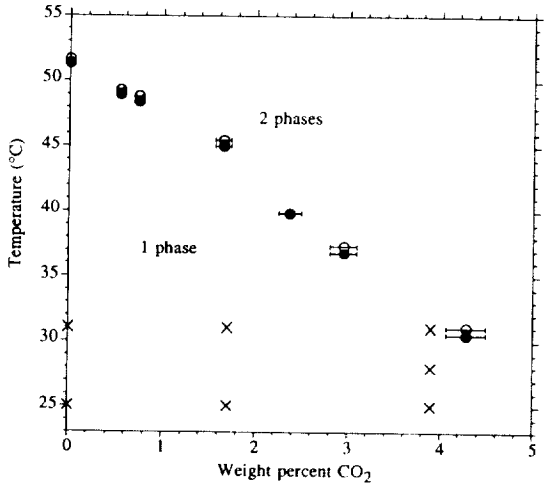

Figure 3. Temperature-composition phase diagrams for $D_2O/CO_2/C_{12}E_6$ mixtures at a constant $D_2O/C_{12}E_6$ weight ratio of 12.8 to 1. Open circles are data at 90.7 bar and the filled circles represent data at 63.1 bar. Crosses show the SANS operating conditions.

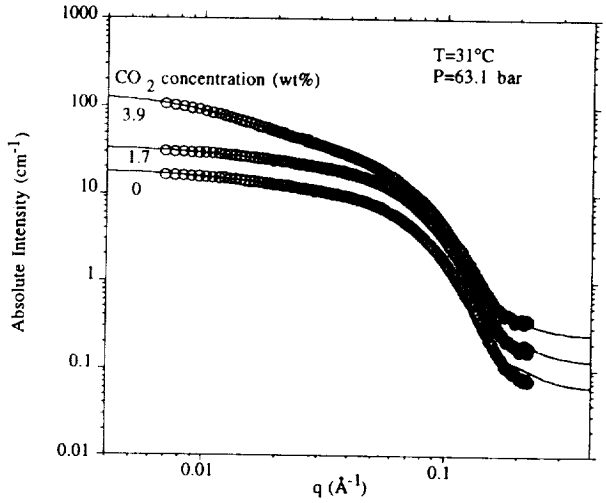

Figure 4. SANS spectra of solutions at 31°C and 63.1 bar for solutions at a constant CO_2 concentrations of 0, 1.7 (x2), 3.9 (x4) wt% CO_2 and constant $D_2O/C_{12}E_6$ weight ratio of 12.8 to 1. There is a large intensity increase at low q at the highest CO_2 concentration. Lines represent model fits to the data.